Eur. Phys. J. B **38**, 19–24 (2004)
DOI: 10.1140/epjb/e2004-00094-0

THE EUROPEAN PHYSICAL JOURNAL B

Intensity and wavelength dependence of the photoconductivity in Cr-doped $Sr_{0.61}Ba_{0.39}Nb_2O_6$

U. Dörfler[1], T. Granzow[1,a], Th. Woike[1], M. Wöhlecke[2], M. Imlau[2], and R. Pankrath[2]

[1] Institute for Mineralogy, University of Cologne, Zülpicherstr. 49b, 50674 Cologne, Germany
[2] Department of Physics, University of Osnabrück, Barbarastr. 7, 49069 Osnabrück, Germany

Received 28 July 2003 / Received in final form 18 December 2003
Published online 20 April 2004 –

Abstract. We examine the light-induced charge transport properties of a series of chromium-doped $Sr_{0.61}Ba_{0.39}Nb_2O_6$ single crystals by measurements of the optical absorption and the electric conductivity. By comparing the wavelength dependence of the specific photoconductivity and the optical absorption we show that both effects stem from the same center. The intensity dependence of the photoconductivity shows the applicability of a one-center charge transport model for high doping concentrations, while for low doping concentrations a more sophisticated model is needed. The validity of a one-center model is exemplarily verified for a crystal doped with 0.51 mol % Cr over a wide intensity range using a holographic method. The product of mobility and recombination time of photoexcited electrons is deduced from the specific photoconductivity.

PACS. 72.40.+w Photoconduction and photovoltaic effects – 72.80.Sk Insulators – 77.84.Dy Niobates, titanates, tantalates, PZT ceramics, etc.

1 Introduction

The relaxor-ferroelectric strontium-barium-niobate (SBN, $Sr_{0.61}Ba_{0.39}Nb_2O_6$) has received wide attention due to its interesting nonlinear optical properties. Applications in the field of holographic data storage seem especially promising, since SBN is the first material that allows an all-electrical fixing of holograms [1–3]. For photorefractive applications, special attention was given to SBN doped with rare earth elements such as cerium or transition metals such as chromium, since doping increases the electrooptic coefficients [4,5], enhances the photorefractive sensitivity in the blue spectral range [6] and extends it to the red [7]. Compared to Ce doping, doping with Cr speeds up the photorefractive response [8]. Cr-doped crystals have an advantage over Ce-doped crystals in holographic applications, because they show no significant beam fanning. The charge transport mechanism in SBN:Ce has been extensively studied [9–11], while less studies have been devoted to the charge transport in SBN:Cr [12]. Measurements of the temporal development of the refractive index modulation during hologram writing hint at a strong dependence of the charge transport mechanism on the doping concentration in SBN:Cr [13] and suggest the possibility that more centers than the well-known Cr^{3+}/Cr^{4+} contribute to the charge transport.

In this work we present measurements of the photoconductivity σ_{ph} as a function of light intensity and wavelength for a series of Cr-doped SBN crystals. The results are compared with those obtained from optical absorption measurements. The photoconductivity σ_{ph} is determined both by the conventional method of measuring the electric current through an illuminated sample and by the holographic method of measuring the decay time of holographic gratings under homogeneous illumination. From the specific photoconductivity, σ_{ph}/I, values for the product of the mobility and the recombination time of the charge carriers, $\mu \cdot \tau_{\mathrm{R}}$, are determined where applicable. We discuss the results with respect to the nature of the photorefractive centers.

2 Theory

When two spatially and temporally coherent plane light waves with the wavelength λ and the wavevectors $\mathbf{k}_1$ and $\mathbf{k}_2$ impinge under an angle θ on a crystal, they interfere, forming a sinusoidal light intensity pattern of bright and dark regions. If movable charges are excited by the light, this inhomogeneous intensity distribution will cause the formation of a sinusoidal elementary space charge field grating with the amplitude $\mathbf{E}_{\mathrm{sc}}$:

$$\mathbf{E}(\mathbf{r}) = \mathbf{E}_{\mathrm{sc}} \cdot \sin(\mathbf{K} \cdot \mathbf{r} + \varphi), \tag{1}$$

[a] e-mail: granzow@linux23.kri.uni-koeln.de

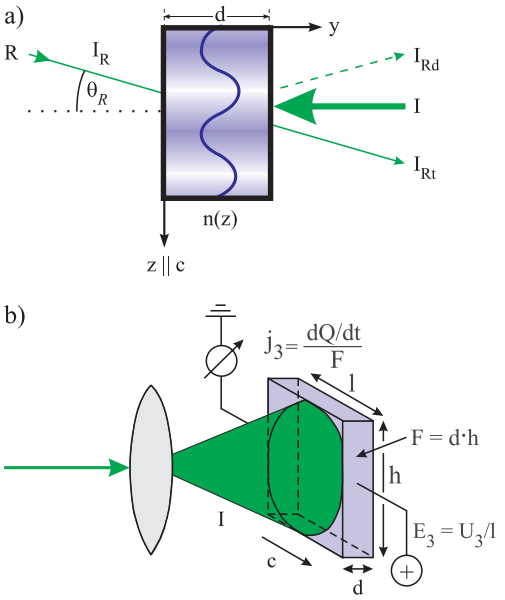

Fig. 1. Measurement of the conductivity by means of (a) the holographic method and (b) the conventional method. For details see the text.

where $\mathbf{K}$=$\mathbf{k}_1$-$\mathbf{k}_2$ is the wavevector of the grating and φ is a phase shift between the light intensity modulation and the space charge field grating caused by the specific charge transport mechanism. In SBN, the charge transport is dominated by the diffusion mechanism, therefore $\varphi = \pi/2$. In an electrooptic crystal, $\mathbf{E}(\mathbf{r})$ will induce a change in the refractive index with the amplitude $\Delta n \propto |\mathbf{E}_{\rm sc}|$. If the resulting refractive index grating is illuminated with only one of the writing beams, e.g. the reference beam (Fig. 1a), a fraction $I_{\rm Rd}$ of the beam intensity is diffracted, while another fraction $I_{\rm Rt}$ passes the crystal undisturbed. The amplitude Δn of the refractive index change is connected with the diffraction efficiency $\eta = I_{\rm Rd}/(I_{\rm Rd} + I_{\rm Rt})$ via the equation

$$\eta = \sin^2\left(\frac{\pi\, d\, \Delta n}{\lambda\, \cos\theta}\right), \tag{2}$$

where d is the thickness of the hologram, which in thin samples is generally equal to the sample thickness.

Without the writing beams, the electric conductivity $\hat{\sigma}$ causes a current $\mathbf{j} = \hat{\sigma}\,\mathbf{E}$ according to Ohm's law. The continuity equation $\nabla\mathbf{j} = -\dot{\rho}$ connects $\mathbf{j}$ with the charge density ρ, and Maxwell's first equation $\rho = \varepsilon_0\nabla(\hat{\varepsilon}\mathbf{E})$ does the same for ρ and $\mathbf{E}$ via the dielectric tensor $\hat{\varepsilon}$ of the crystal and that of the vacuum ε_0. Taking into account the commutability of space and time derivatives, we arrive at

$$\dot{E}_{\rm sc,3} = -\frac{\sigma_{33}}{\varepsilon_{33}\varepsilon_0}\, E_{\rm sc,3}. \tag{3}$$

Thus, the space charge field decays exponentially according to

$$E_{\rm sc,3}(\mathrm{t}) = E_{\rm sc,3}(0)\, \exp\left(-\frac{t}{\tau_{\rm M}}\right) \tag{4}$$

with Maxwell's relaxation time $\tau_{\rm M} = (\varepsilon_{33}\varepsilon_0)/\sigma_{33}$. Since Δn is proportional to $E_{\rm sc,3}$ at any time, the refractive index grating decays with the same $\tau_{\rm M}$. If the dielectric constant ε_{33} of the crystal is known, one can thus calculate the electric conductivity σ_{33} by measurements of the temporal development of Δn. If the crystal is not illuminated, $\sigma_{33} = \sigma_{\rm d}$ is the dark conductivity of the crystal. If the hologram is erased by a homogeneous illumination of the crystal, σ_{33} is equal to the sum of $\sigma_{\rm d}$ and the photoconductivity $\sigma_{\rm ph}$. If only one center with two different valence states is responsible for the photoexcitation of charges, $\sigma_{\rm ph}$ is given by [10]

$$\sigma_{\rm ph} = \frac{e\lambda\cdot\alpha\mu\tau_{\rm R}}{\mathrm{h}c} I =: \Sigma I, \tag{5}$$

with the optical absorption coefficient α, the mobility μ and recombination time $\tau_{\rm R}$ of the excited charges, the specific photoconductivity $\Sigma = \sigma_{\rm ph}/I$ and the light intensity I. If $\sigma_{\rm ph}(I)$ is measured, one can thus determine the product $\mu\tau_{\rm R}$ from the specific photoconductivity:

$$\mu\cdot\tau_{\rm R} = \frac{\mathrm{h}c}{e\lambda\alpha}\cdot\left(\frac{\sigma_{\rm ph}}{I}\right). \tag{6}$$

If more than one center or more than two valence states are involved in the photoinduced charge transport, the photoconductivity can empirically be described as a nonlinear function of the light intensity [14]:

$$\sigma_{\rm ph} \propto I^{\rm x} =: \Sigma_x I^{\rm x} \tag{7}$$

with the exponent $0 \le x \le 1$ and a specific photoconductivity Σ_x. Note, that for $x = 1$ equation (7) corresponds to equation (5).

3 Experimental details

For our measurements we used single crystals of SBN grown by the Czochralski technique. Chromium doping was performed by adding certain amounts of Cr_2O_3 into the melt. The coefficient for the incorporation of the doping ions was taken from reference [13]. All samples were cuboids with dimensions of approximately $5 \times 1 \times 5$ mm^3 along the crystallographic a-, b- and c-axis, respectively. The optical absorption coefficients $\alpha(\lambda)$ of all samples were measured for both ordinary and extraordinary light polarization with a Cary-17D spectrometer.

To measure the electric conductivity σ_{33} conventionally, a sample was placed in a temperature controlled holder assuring a temperature stability of 1 °C. The setup is shown in Figure 1b. The two c-faces of the sample were connected to a charge amplifier and a high voltage power supply, respectively. When an electric field E_3 was applied parallel to the c-axis, the resulting charge change ΔQ was measured. Since the dimensions of the sample were known, the time derivative dQ/dt together with the area F gave the current density j_3. The corresponding element of the conductivity tensor was determined according to $j_3 = \sigma_{33}\cdot E_3$. In a first step, the applicability of Ohm's law was tested by applying various external fields between 0 V/mm and 400 V/mm to

the unilluminated sample and measuring $j_3(E)$. The sample was then homogeneously illuminated by a frequency-doubled Nd:YAG laser ($\lambda = 532$ nm). The intensity and polarization direction of the light could be adjusted by a half-wave retarder plate and a Glan-Thompson prism. A light intensity between 0 and 120 mW/cm^2 was set, a field $E_3 = 200$ V/mm was applied, and j_3 was measured for five minutes before the light intensity was changed and the cycle started anew.

To measure the wavelength dependence of σ_{33}, the crystal was illuminated with a high pressure xenon lamp. Wavelength selection was performed with an accuracy of 10 nm using a grating monochromator, the light intensity was adjusted with neutral density filters. Starting at $\lambda = 770$ nm, j_3 was measured for different intensities for an external field of $E_3 = 200$ V/mm. The wavelength λ was then decreased by 10 nm and the cycle repeated until $\lambda = 420$ nm was reached.

The holographic measurements were performed with a typical two-beam coupling setup: The laser beam was divided by a beam splitter into a signal and a pump wave, which coincided under an angle of $\theta = 20°$ and interfered on the sample. Intensity and polarization of the incoming light were adjusted by half-wave retarder plates and Glan-Thompson prisms. The intensity ratio between pump and signal beam was 1000:1 to guarantee measurements in the undepleted pump regime. The intensities of both beams were detected behind the crystal by two Si-photodiodes. A diffraction grating was written until a saturation state was reached. The grating was then erased by illumination with an off-Bragg erasure beam originating from the same laser source as the writing beams (Fig. 1a). The diffracted intensity of the weak signal beam was used to monitor the erasure process as a function of the erasure intensity and time. In order to avoid hologram writing by interference of the erasure beam and the monitor beam, orthogonal light polarization was used.

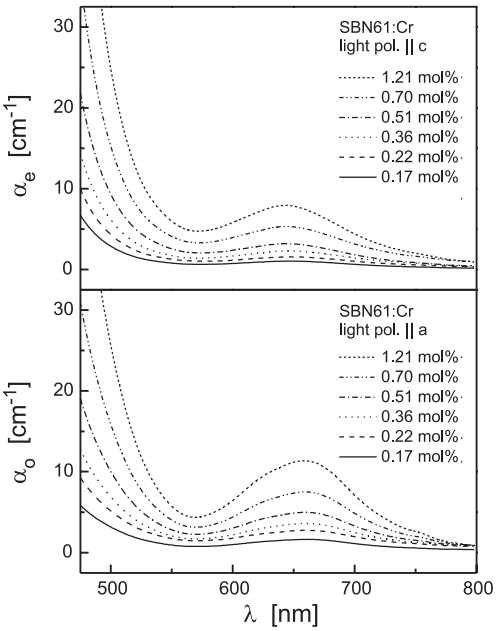

Fig. 2. Absorption spectra of SBN:Cr with different doping concentrations for both extraordinarily (α_e) and ordinarily (α_o) polarized light.

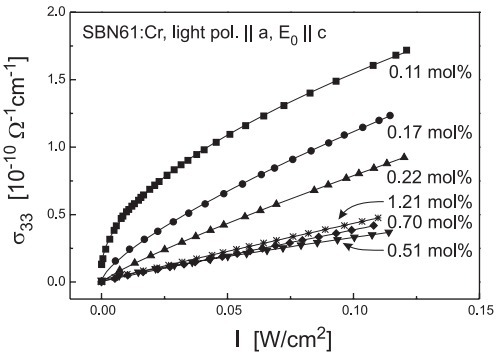

Fig. 3. Intensity dependence of the conductivity σ_{33} for SBN:Cr with different doping concentrations at $\lambda = 532$ nm and ordinary light polarization. The continuous lines represent fits of equation (7) to the data.

4 Experimental results

Figure 2 shows the extraordinary and ordinary absorption coefficient α_e and α_o, respectively, for a series of SBN:Cr with different doping concentrations. Because of the well-known transition of Cr^{3+} within a spin-quartet all spectra show a maximum at about 650 nm. The maximum increases with increasing doping concentration. Parallel to this increase of α, the onset of the fundamental absorption edge in the blue-green spectral range is shifted to higher wavelengths. Note that $\alpha(\lambda)$ is proportional to c_{Cr} for both spectral ranges, independent of the wavelength.

Figure 3 shows the results of measurements of $\sigma_{33}(I)$ at a single wavelength $\lambda = 532$ nm for several SBN:Cr. The continuous lines represent the results of a fit of equation (7) to the data sets, where the dark conductivity σ_d, the specific photoconductivity Σ_x and the exponent x are fitting parameters. It is obvious from Figure 3 that the conductivity at first strongly decreases with increasing doping concentration c_{Cr} until $c_{Cr} = 0.51$ mol% is reached, and then starts to rise again very slowly. This behavior coincides with a notable change in the curve shapes: While $\sigma_{33}(I)$ remarkably deviates from a linear behavior at low c_{Cr}, it becomes nearly linear for the two highest values of c_{Cr}. This is also reflected in the exponent x, which rises from 0.58 to almost unity.

Figure 4 shows the dark conductivity σ_d as a function of c_{Cr}. We obtained σ_d as axis intercept of the sublinear fits to $\sigma_{33}(I)$. It shows a strong decrease for $0 \leq c_{Cr} \leq 0.11$ mol% and saturates for $c_{Cr} \geq 0.17$ mol%.

To compare the photoconductivity with the optical absorption, which reflects the charge transport process, we measured the wavelength dependence of the specific photoconductivity Σ_x by direct detection of the electric current. Figure 5 exemplarily shows $\Sigma_x(\lambda)$ for two doping concentrations for ordinarily polarized light. The λ-dependence of Σ_x clearly mirrors that of the optical

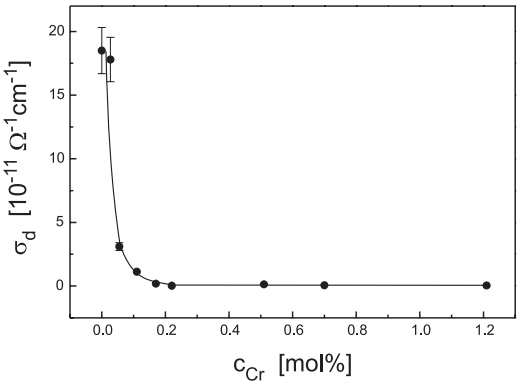

Fig. 4. Dark conductivity $\sigma_{\rm d}$ in dependence on the chromium concentration. The line is a guide for the eyes.

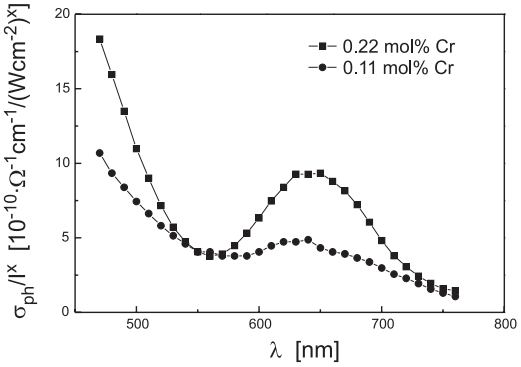

Fig. 5. Σ_x=σ_{ph}/I^x as a function of λ for SBN:Cr 0.11 mol % and 0.22 mol % at ordinary light polarization. Each data point results from a sublinear fit to $\sigma_{33}(I)$ (Fig. 3).

absorption, the most prominent features being the local maximum at $\lambda \approx 650$ nm and a strong increase for lower wavelengths where fundamental absorption sets in.

Together with the values of the optical absorption $\alpha_{\rm o}$ at $\lambda = 532$ nm from Figure 2, the product of mobility μ and recombination time $\tau_{\rm R}$ of the electrons was determined from Σ for $x = 1$ according to equation (6). We obtained $\mu\tau_{\rm R} = (1.36 \pm 0.04) \times 10^{-10}$ cm^2/V for $c_{\rm Cr} = 0.70$ mol % and $\mu\tau_{\rm R} = (0.94 \pm 0.02) \times 10^{-10}$ cm^2/V for $c_{\rm Cr} = 1.21$ mol %, independent of the light intensity. Note that the intensity dependence of the conductivity showed a linear behavior only for these two concentrations. For non-linear dependencies of $\sigma_{\rm ph}$ on I the product $\mu\tau_{\rm R}$ is a function of I. Two values are exemplarily shown in Table 1 for intensities of 0.1 W/cm^2 and 0.01 W/cm^2. As expected, $\mu\tau_{\rm R}$ shows a general decrease with increasing $c_{\rm Cr}$ at a given light intensity. Since $x < 1$, $\mu\tau_{\rm R}$ also decreases with increasing I at a given doping concentration. Of course, this decrease is lower the closer x is to unity.

The holographic method did not require the illumination of the entire crystal from one electrode to the other, but merely that of the small spot where the holographic grating was written. It thus allowed us to reach even higher values of the light intensity than the conventional electrical measurement technique. For the crystal

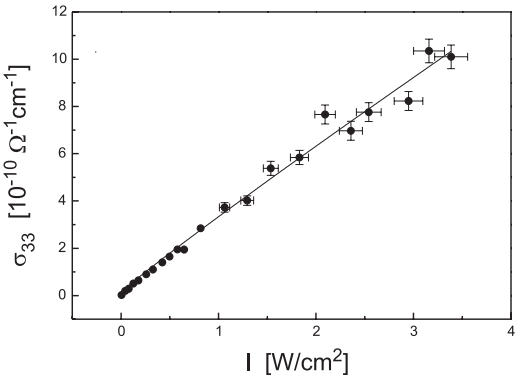

Fig. 6. $\sigma_{33}(I)$ determined from the erasure of holographic gratings at $\lambda = 532$ nm and ordinary light polarization in SBN:Cr (0.51 mol %). Note that the probe and the erasure beam were orthogonally polarized. The dark conductivity was taken from the conventional measurement and fixed during the fit.

Table 1. Product of mobility μ and recombination time $\tau_{\rm R}$ of the electrons for a nonlinear dependence $\sigma_{33}(I)$ for $I = 0.1$ W/cm^2 and $I = 0.01$ W/cm^2.

$c_{\rm Cr}$ [mol %]	0.055	0.11	0.17	0.22	0.51
$\mu\tau_{\rm R}$ [10^{-9} cm^2/V] ($I = 0.1$ W/cm^2)	11	5.8	1.8	0.75	0.18
$\mu\tau_{\rm R}$ [10^{-9} cm^2/V] ($I = 0.01$ W/cm^2)	38	19	3.7	1.0	0.37

doped with 0.51 mol % Cr, $\Delta n(t)$ showed an exponential decay behavior under illumination, as predicted by theory. Figure 6 shows the values of σ_{33} determined from the time constant $\tau_{\rm M}$ of this decay versus the light intensity I for SBN:Cr (0.51 mol %) at a wavelength of $\lambda = 532$ nm. The value $\varepsilon_{33} = (2000 \pm 100)$ of the dielectric constant was estimated from measurements of the hysteresis curve as described in reference [15] for SBN61:Ce. The holographically determined conductivity shows a comparable behavior over I as the one obtained from electrical measurements: The exponent x from fitting a sublinear function to the measured holographic data amounts to $x = 0.95$, which is close to a curve linearity. The specific photoconductivity is determined to be $(3.2 \pm 0.1) \times 10^{-10}$ cm/V^2. As a result, the product $\mu\tau_{\rm R}$ is calculated to be 1.76×10^{-10} cm^2/V.

5 Discussion

The absorption spectra in Figure 2 clearly show that increasing the doping concentration raises the number of photorefractive Cr^{3+} centers, thus raising both $\alpha_{\rm o}$ and $\alpha_{\rm e}$ [16]. In addition our results confirm the results of Vikhnin et al. [17] for $\alpha_{\rm o}$ of the $^4T_1 \rightarrow {}^4T_2$ transition at $\lambda = 650$ nm and extend them with respect to the chromium-induced transition at the onset of the band edge. This absorption scales with the chromium concentration, and studies of the composition dependence of the

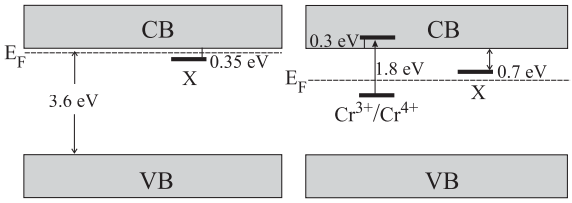

Fig. 7. Model for the microscopic charge transport in (a) undoped SBN and (b) SBN:Cr.

band edge of undoped SBN revealed an unspectacular shift due to compositional disorder [18]. Therefore we attribute this absorption to transitions from $^4T_1$ to higher excited Cr levels but not to the onset of band-band transitions.

The measurement of the wavelength dependence of the specific photoconductivity $\Sigma_x = \sigma_{ph}/I^x$ showed a strong dependence of the exponent x on the doping concentration: we obtained, e.g. $x = 0.55$ ($\lambda = 532$ nm, 0.11 mol % Cr) and $x = 0.86$ ($\lambda = 532$ nm, 0.22 mol % Cr), i.e. $\sigma_{ph}(I)$ is sublinear for both doping concentrations. This makes a comparison of Σ_x for differently doped crystals unreasonable. For each sample, x was independent of λ. Qualitatively, $\Sigma_x(\lambda)$ shows the same behavior as $\alpha(\lambda)$, the most prominent feature being the maximum at about 650 nm in the red spectral range. Thus we conclude that both the photoconductivity and the optical absorption stem from the same photorefractive center.

The dark conductivity decreases with increasing c_{Cr} (Fig. 4). The origin of the dark conductivity has not yet been the subject of intensive discussions. However, our experimental findings may yield some valuable information. For an interpretation we propose the following microscopic model, which is depicted in Figure 7 and resembles that introduced by Gao et al. [12] for light-induced charge transfer and kinetics of the NIR absorption of Nb^{4+} polarons in SBN. First of all, we observed a pronounced dependence of the dark conductivity on the chromium concentration, in particular a strong decrease of the conductivity for slightly doping with Cr or Ce. Therefore we have to introduce an unspecified shallow level X, likely of a polaron type.

Within this model in the case of undoped SBN (Fig. 7a) the origin of σ_d is due to a pure thermal excitation of electrons from the shallow level into the conduction band. The Fermi energy E_F is expected slightly above this shallow level below the conduction band. By doping the crystal with chromium, σ_d decreases with increasing c_{Cr}, because the shallow levels are depleted in favor of the Cr levels. Thus, E_F decreases, the energy of the X-level is changed (Fig. 7b) and pure thermal excitations of electrons with respect to the conduction band are greatly reduced.

The energy level of Cr in the gap (Fig. 7b) was derived by subtracting the thermal energy from the optical excitation energy (Fig. 2). To do this we used that the broad and almost symmetrical absorption band of Cr is mainly due to a strong electron-phonon interaction. With an average phonon energy of 300 cm^{-1} [19] and a Huang Rhys factor of 10 we arrive at about 0.3 eV and thus the Cr level has to be placed approximately 1.5 eV below the conduction band edge, see Figure 7.

The activation energy of level X for undoped SBN was deduced from the temperature dependence of the dielectric constant (0.35 eV) and was estimated for Cr-doped SBN from the temperature dependence of the photoconductivity (0.7 eV). For an interpretation of the origin of the X level the adoption of small polarons hopping or tunneling as introduced by Gao et al. [12] is tempting. However, we cannot use this model for the explanation of the dark conductivity. We emphasize that we are dealing besides Cr-doped samples with unreduced undoped SBN were no small polaron absorption is observable at all. Further our activation energies are in each case well above the well known energy of about 0.16 eV for hopping or tunneling deduced as one quarter of the polaron energy. On the other hand we are sure that our undoped crystals contain impurities on a sub ppm level only, but we observe a significant dark current. Therefore we need an intrinsic defect, which is not as mobile as the small Nb^{4+}, but we may stick to polarons, in particular to bound ones. Then our observed activation energy is reasonable and not in contradiction to polaron relations.

The dependence of the exponent x obtained from fitting sublinear functions to $\sigma_{33}(I)$ on the Cr-concentration can be explained by the above mentioned model: For high concentrations of 0.70 and 1.21 mol % Cr a linear behavior was observed. In this case, a thermal excitation of charge carriers is not possible, because the shallow level is depleted and the Cr levels are too deep. Thus, the charge carriers can be solely photoexcited from the photrefractive Cr centers. For weaker concentrations the exponent x ranges from 0.5 to 1. In this case, photoexcitation from both the Cr levels and the shallow levels can take place.

Measurements of the light-induced absorption would be a stronger criterion to distinguish between a one-center model and a two-center or three-valence model [9], but in the case of congruent SBN:Cr only limited data on the light-induced absorption have been reported. Measurements of Gao et al. are restricted to 240 K, weak Cr concentrations of 0.11 mol % and $\lambda = 488$ nm [16]. They found a pronounced light-induced absorption, a result which supports our measurements of the photoconductivity.

A comparison between the conventionally and the holographically measured photoconductivity shows a good agreement. As mentioned above, in the case of the conventional method a linear behavior of the conductivity as a function of the intensity was found for large Cr concentrations of 0.70 mol % and 1.21 mol %, respectively. In the case of the holographic measurements, the crystal doped with 0.51 mol % Cr already shows a linear behavior. The trend to a linear description of the data, i.e., the existence of a one-center model, is supported by both methods. Thus, a limiting Cr concentration of about 0.6 mol % can be deduced. The absolute values for the specific photoconductivity also have comparable order of magnitude: for 0.51 mol % Cr and a wavelength of 532 nm we found conventionally $(2.27 \pm 0.01) \times 10^{10}$ cm/V^2, and holographically $(3.2 \pm 0.1) \times 10^{10}$ cm/V^2. While the conventional

method is more accurate, the holographic method could verify the linearity of $\sigma(I)$ over a larger intensity range (<3.5 W/cm^2 compared to <0.12 W/cm^2).

From the values of the specific photoconductivity the product $\mu\tau_{\mathrm{R}}$ could be calculated when $\sigma(I)$ was linear. Corresponding to the values of the specific photoconductivity, we also get comparable values of $\mu\tau_{\mathrm{R}}$ for both the conventional and the holographic method. Comparison with literature values is difficult, because here we concentrate on examining the charge transport mechanism while most published data are concerned with the speed of grating formation, which is of course of more practical interest. As a consequence, our holographic measurements were performed in the grating erasure mode with homogeneous illumination, which allowed a better comparison with our conventional measurements of the photoconductivity. Furthermore, there are large discrepancies among the published values: Vazquez et al. found by means of a holographic measurement of grating formation rates for $\lambda = 514.5$ nm and a weak dopant concentration between 0.015 wt. % and 0.025 wt. % Cr a linear dependence of the rate $\tau^{-1}(I)$, and thus of $\sigma_{33}(I)$ [20], in contrast to the results presented in this work. From that, a value of $\mu\tau_{\mathrm{R}} = 53.6 \times 10^{-10}$ cm^2/V is determined. The value of $\sigma_d = 5.51 \times 10^{-10}\ \Omega^{-1}\,\mathrm{cm}^{-1}$ is larger by a factor of 2 than the value determined in this work. Tomita and Suzuki determine also from holographic measurements of the grating formation rates a value of $\mu\tau_{\mathrm{R}} = 7.2 \times 10^{-13}$ cm^2/V for $\lambda = 514.5$ nm and 12.6×10^{-13} cm^2/V for $\lambda = 632.8$ nm for a sample doped with 0.02 wt. % Cr [7]. These values are smaller by more than three orders of magnitude than the values found by Vazquez et al. The values of the dark conductivity of $\sigma_d = 9.0 \times 10^{-10}\,\Omega^{-1}\,\mathrm{cm}^{-1}$ (from a linear fit to the data for $\lambda = 514.5$ nm) and $4.7 \times 10^{-10}\,\Omega^{-1}\,\mathrm{cm}^{-1}$ (from a linear fit to the data for $\lambda = 632.8$ nm) have the same order of magnitude as our values. Comparing our values to the literature data, the main difference is that we found a dependence of the charge transport parameters on c_{Cr}, because we systematically examined a series of Cr doped crystals with well-known Cr concentrations in the crystal, referring to our previous investigations [13].

This work was supported by the Deutsche Forschungsgemeinschaft (SPP 1056 Wo 618/3-4; Graduate College 695) and INTAS (01-0173). We thank K. Buse (University of Bonn) for the possibility to measure the optical absorption.

References

1. F. Micheron, G. Bismuth, Appl. Phys. Lett. **20**, 79 (1972)
2. F. Micheron, G. Bismuth, Appl. Phys. Lett. **23**, 71 (1973)
3. Y. Qiao, S. Orlov, D. Psaltis, R.R. Neurgaonkar, Opt. Lett. **18**, 1004 (1993)
4. R.A. Vazquez, F.R. Vachss, R.R. Neurgaonkar, M.D. Ewbank, J. Opt. Soc. Am. B **8**, 1932 (1991)
5. U.B. Dörfler, R. Piechatzek, Th. Woike, M.K. Imlau, V. Wirth, L. Bohatý, T. Volk, R. Pankrath, M. Wöhlecke, Appl. Phys. B **68**, 843 (1999)
6. K. Megumi, H. Kozuka, M. Kobayashi, Y. Furuhata, Appl. Phys. Lett. **30**, 631 (1977)
7. Y. Tomita, A. Suzuki, Appl. Phys. A **59**, 579 (1994)
8. K. Sayano, A. Yariv, R.R. Neurgaonkar, Appl. Phys. Lett. **55**, 328 (1989)
9. K. Buse, U. van Stevendaal, R. Pankrath, E. Krätzig, J. Opt. Soc. Am. B **13**, (1996) 1461
10. K. Buse, Appl. Phys. B **64**, 273 (1997)
11. K. Buse, A. Gerwens, S. Wevering, E. Krätzig, J. Opt. Soc. Am. B **15**, 1674 (1998)
12. M. Gao, S. Kapphan, S. Porcher, R. Pankrath, J. Phys.: Condens. Matter **11**, 4913 (1999)
13. Th. Woike, U. Dörfler, L. Tsankov, G. Weckwerth, D. Wolf, M. Wöhlecke, T. Granzow, R. Pankrath, M. Imlau, W. Kleemann, Appl. Phys. B **72**, 661 (2001)
14. L. Holtmann, Phys. Status Solidi (a) **113**, K89 (1989)
15. T. Granzow, U. Dörfler, Th. Woike, M. Wöhlecke, R. Pankrath, M. Imlau, Phys. Rev. B **63**, 174101 (2001)
16. Ming Gao, S. Kapphan, R. Pankrath, Xiqi Feng, Yuanfen Tang, V. Vikhnin, J. Phys. Chem. Solids **61**, 1775 (2000)
17. V.S. Vikhnin, I. Kislova, A.B. Kutsenko, S.E. Kapphan, Solid State Commun. **121**, 83 (2002)
18. C. David, M. Ulex, A. Tunagy, M. Wöhlecke, K. Betzler, to be published (2004)
19. M. Meyer, M. Wöhlecke, O.F. Schirmer, Phys. Status Solidi (b) **221**, R1 (2000)
20. R.A. Vazquez, M.D. Ewbank, R.R. Neurgaonkar, Opt. Commun. **80**, 253 (1991)